Swarm-IPIR Description of the Processing Algorithm

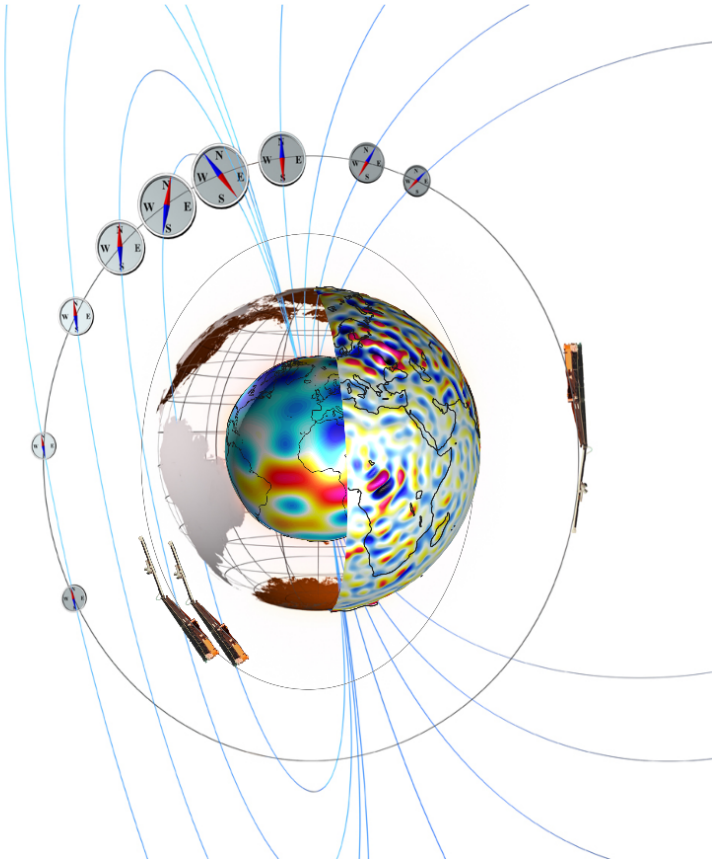

Doc. no: SW-TN-UiO-GS-004, Rev: 1 dA, 10 June 2018

Prepared:

Yaqi Jin Date 05 May 2018

Scientist

Prepared:

Chao Xiong Date 10 June 2018

Scientist

Approved:

Wojciech J. Miloch Date 05 May 2018

Project Manager

Record of Changes

Reason	Description	Rev	Date
Initial vers.	Released	1 dA	10 June 2018

Table of Contents

1 Introduction

1.1 Scope and applicability

This document comprises the Swarm Level 2 (L2) IPIR product Validation Report (VR) document for the Swarm Data, Innovation and Science Cluster (Swarm DISC) consortium in response to the requirements of [AD-1]. Swarm-IPIR includes the following products [AD-4]:

- EFIx_PL_1B – 2Hz data from the Electrical Field Instrument (EFI).
- TECxTMS_2F – TEC data derived from onboard GPS.
- AOBxFAC_2F – Auroral Oval Boundaries (AOB) using the Field-Aligned Current (FAC) method.
- IBIxTMS_2F, IBI: Ionospheric Bubble Index.
- Polar Cap Products (PCP).

The Swarm-IPIR Product Definition document [AD-4] is available in the SVN folder: https://smart-svn.space-center.dk/svn/smart/SwarmDISC/DISC_Projects/ITT1_4_ionospheric_irregularities/Deliverables/.

Current or updated version of this document is available in the SVN folder: https://smart-svn.space-center.dk/svn/smart/SwarmDISC/DISC_Projects/ITT1_4_ionospheric_irregularities/Deliverables/.

2 Applicable and Reference Documentation

2.1 Applicable Documents

The following documents are applicable to the definitions within this document.

[AD-1] SW-SW-DTU-GS-114, rev 1 Statement of Work for Swarm DISC ITT 1.4 “Ionospheric irregularities and fluctuations based on Swarm data”

[AD-2] IPIR-Swarm-IPIR-12017 – Ionospheric Plasma IRregularities characterised by the Swarm satellites.

[AD-3] https://earth.esa.int/web/guest/missions/esa-eo-missions/swarm/data-handbook

[AD-4] SW-TN-UiO-GS-001, Swarm-IPIR Product Definition.

[AD-5] SW-TN-UiO-GS-003, Swarm-IPIR Description of the Processing Algorithm.

2.2 Reference Documents

The following documents contain supporting and background information to be taken into account during the activities specified within this document.

[RD-1] SW-TN-UiO-GS-003, Swarm-IPIR Description of the Processing Algorithm.

[RD-2] Crowley, G., A. J. Ridley, D. Deinst, S. Wing, D. J. Knipp, B. A. Emery, F. Foster, R. Heelis, M. Hairston, and B. W. Reinisch (2000), Transformation of high-latitude ionospheric F region patches into blobs during the March 21, 1990, storm, J. Geophys. Res., 105, 5215–5230, doi:10.1029/1999JA900357.

2.3 Abbreviations

Acronym ***or abbreviation***	***Description***
AOB	Auroral Oval Boundaries
DISC	The Data, Innovation and Science Cluster
DPA	Description of the Processing Algorithm
FAC	Field-Aligned Current
GFZ	The Helmholtz Centre Potsdam - GFZ German Research Centre for Geosciences, DE
L1b	Level 1b (satellite data)
L2	Level 2 (satellite data)
MLAT	Magnetic Latitude
SVN	SVN Repository with server located at DTU. Presently, the following URLs apply: https://smart-svn.spacecenter.dk/svn/smart/SwarmDISC/DISC_Projects/ITT1_4_ionospheric_irregularities/Deliverables/
Swarm	Constellation of 3 ESA satellites, https://earth.esa.int/web/guest/missions/esa-operational-eo-missions/swarm
TBD	To Be Defined
UiO	The University of Oslo, Oslo, Norway
GISTM	GNSS Ionospheric Scintillation and TEC Monitor

3 Rationale and background

This document provides a validation report for the IPIR-product, which characterises plasma density fluctuations and irregularities encountered by Swarm in terms of their spatial occurrence and amplitudes. This can be analysed relative to the local plasma conditions, i.e., to the local background. IPIR also relates the fluctuations to the ionospheric current system and variations in the magnetic field, in order to relate these structures to dynamic phenomena in the ionosphere. Finally, it combines data from the GPS receivers, where TEC and ROT provide information on the extent of the structures in the direction towards GPS satellites.

The data is acquired from the following instruments onboard Swarm: Electric Field Instrument, which includes the Langmuir probe (LP) and Thermal Ion Imager (TII), magnetometers and GPS antennas. Location of instruments is given in Figure 1.

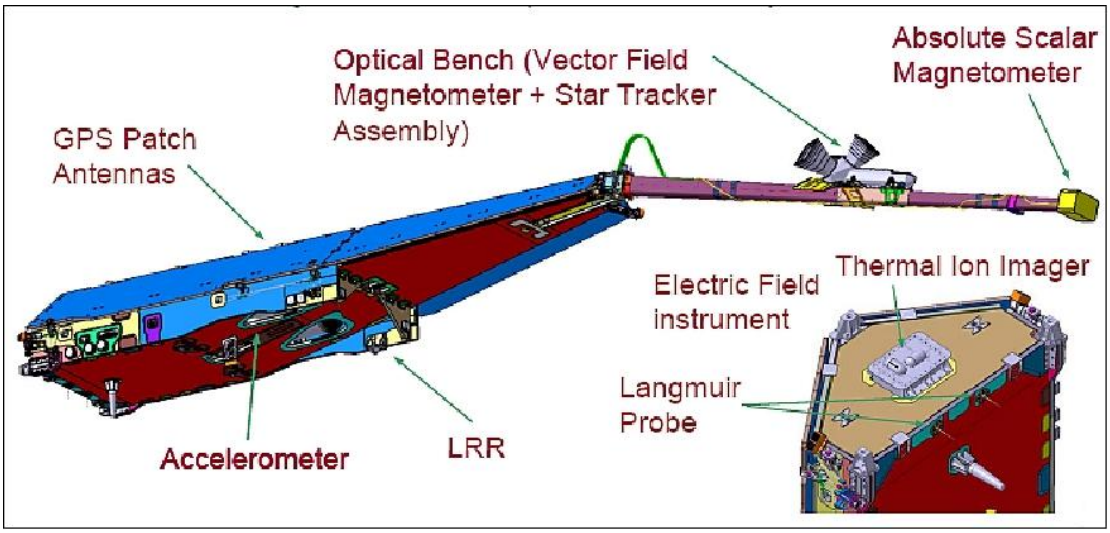

Fig. 1. Swarm satellite with its scientific instruments (Courtesy of ESA).

Based on Swarm data, in the IPIR product, we derive the following parameters, whose definition can be found in the Swarm-IPIR Description of the Processing Algorithm [RD-01]:

- Rate of change of density (ROD),
- Rate of change of density index in 10 seconds (RODI10s),
- Rate of change of density index in 20 seconds (RODI20s),
- filtered *Ne* fluctuations in 10 seconds (delta_Ne10s),
- filtered *Ne* fluctuations in 20 seconds (delta_Ne20s),
- filtered *Ne* fluctuations in 40 seconds (delta_Ne40s),
- *Ne* gradient in 100 km scale (Grad_Ne@100km),
- *Ne* gradient in 50 km scale (Grad_Ne@50km),
- *Ne* gradient in 20 km scale (Grad_Ne@20km),
- *Ne* gradient near the edge of a polar cap patch (Grad_Ne@PCP_edge),
- Rate of change of TEC (*ROT*),
- Rate of change of TEC index (*ROTI*).

In the report we compare the satellite derived data with data from ground-based stations of selected GNSS Ionospheric Scintillation and TEC Monitors (GISTMs). With these ground-based receivers we can monitor the following quantities:

- GPS phase and amplitude scintillation indices (σ_ϕ and S_4), minutely values,
- TEC along the receiver-satellite pair, minutely value,
- ROT and ROTI from the TEC data.

A typical set-up of the GISTM receiver is given in Figure 2,

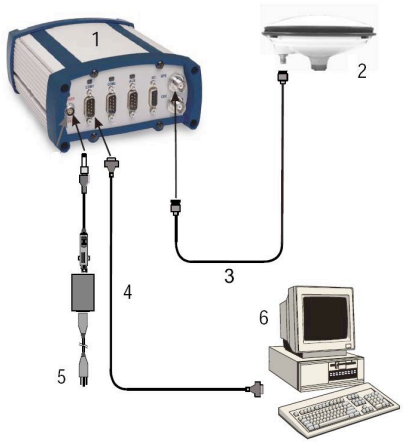

Fig. 2. Typical GISTM receiver consisting of 1) processing unit, 2) receiving antenna, 3-5) cabels and interfaces, 6) computer.

IPIR includes several other parameters in the dataset, such as PCP-index, IBI-flag, Te (electron temperature), Ne (electron density), which have already been validated through a development of other products. In this VR we therefore focus on the new parameter ROD, and also TEC and ROT calculated onboard Swarm, as we can compare those to a different dataset. Derived quantities such as *Ne* fluctuations and gradients are derived from *Ne* using a standard approach as described in [RD-01], and thus cannot be directly compared to independent measurements of the same quantity.

4 Comparison with ground-based GPS scintillation receivers

4.1 Overview of GISTM receivers

In this VR, we make use of 3 selected GISTM receivers to cover the polar cap, auroral and equatorial regions, as these are the regions of different characteristics characterised by different processes in the ionosphere. The locations together with their respective field-of-view are shown in Fig. 3. The locations of the host stations are given in Table 1. We will use in the following only data from GPS satellies.

Site name	Location	(Latitude, Longitude)
NYA	Ny-Ålesund, Svalbard	(78.92°N, 11.93°E)
SKN	Skibotn, Norway	(69.43°N, 20.38°E)
SZT	ShenZhen, China	(22.6°N, 114.0°E)

Table 1. Locations of 3 GISTM receivers used for validation.

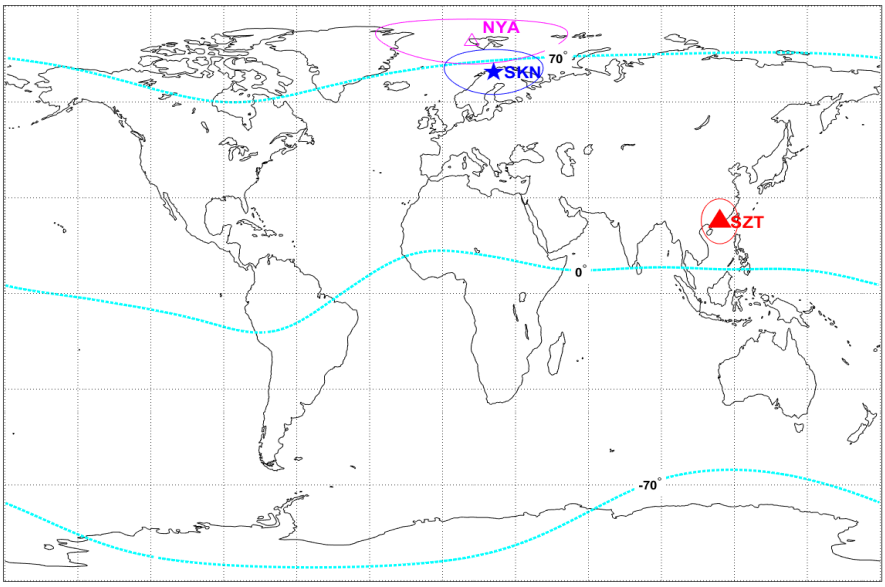

Fig. 3. Location of GISTM receivers presented in this validation report.

4.2 Conjunction with the polar cap station at Ny-Ålesund (NYA)

In order to compare IPIR products with ground-based GPS data, we need to find time intervals when Swarm satellites pass over the field-of-view of the ground-based GPS receiver. To give a sense of the conjunction geometry, we show in Fig. 4 an example of the conjunction between the Swarm A and the ground-based GPS scintillation receiver at Ny-Ålesund on Feb. 9, 2015 at around 22 UT. The left panels in Fig. 4 show observations from Swarm A. For simplicity, we did not plot all parameters from the IPIR dataset.

Fig. 4a-4b show the parameters derived from the electron density (*Ne*). The background electron density is derived by using a 35 percentile filter in a running window of 551 data points, which corresponds to a distance of about 2000 km travelled by the satellite (the sampling frequency being 2 Hz and the velocity of

the satellites being about 7.5 km/s). In order to show the detection of a polar cap patch, we also plot 2 times the background density in magenta as the polar cap patches are often defined as at least two times the background electron density in the polar cap [Crowley et al., 1996]. From the presented dataset we observe that one polar cap patch was detected by Swarm A around 22:02.35 UT. Worth noticing are NYA data from satellites PRN6 and PRN20, which correspond to second half of time interval presented for Swarm. ROT measured for both satellites shows relatively large variations, which one can directly relate to ROD, ROT, and even a small enhancement in the phase scintillation index.

To make the long-term statistics of the conjunction observation, we use data from September to December of 2014 at Ny-Ålesund. Fig. 5 show the scatter plots of VTEC from Ny-Ålesund versus VTEC and electron density from Swarm A. We only use data when the Swarm satellite passed over the field-of-view (indicated with a red circle in Fig. 4f) for more than 60 s. In the scatter plot, one circle in each plot represents one conjunction in the same manner as Fig. 4. It is clear that both density and VTEC measured from space show good correlation with the VTEC observation from ground. A linear fit is shown in each panel in a red line where the linear fit coefficient is shown on the top left of each panel. Thus, there is a good linear relationship between the two datasets.

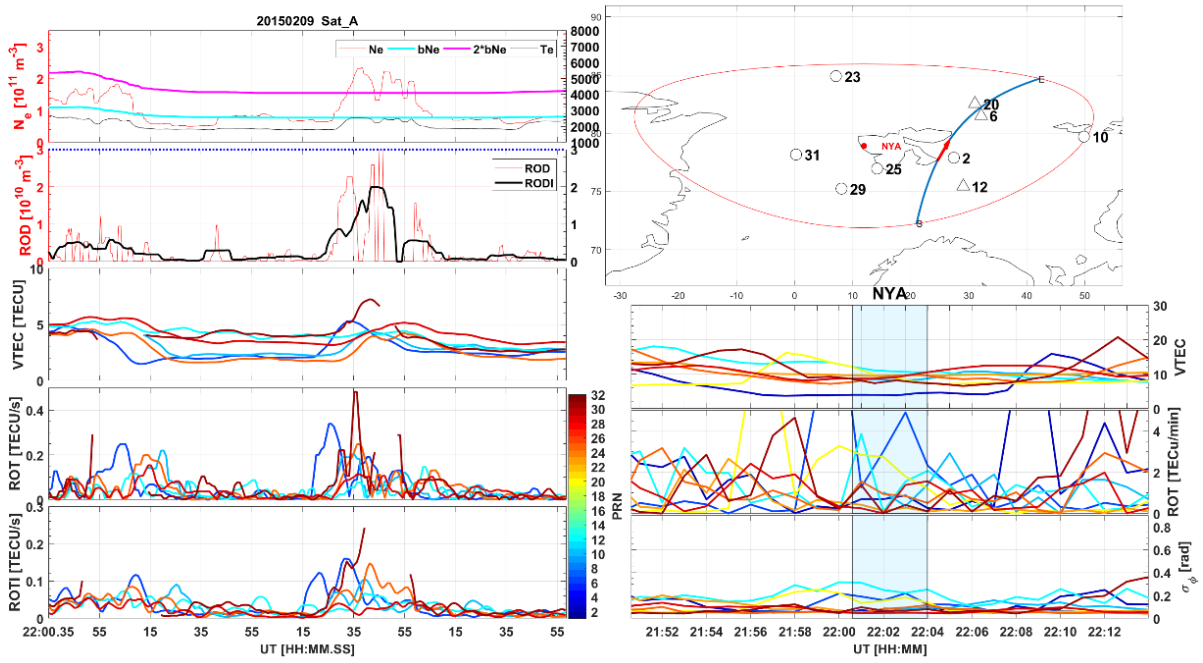

*Fig. 4. An example of the conjunction of Swarm A and the ground-based GPS scintillation receiver at Ny-Ålesund. (a-e) shows the data from Swarm A. (a) The electron density (Ne, red), background electron density (bNe, cyan), 2 times the background density (2*bNe, cyan), and electron temperature (Te, black). (b) The rate of change of density (ROD) and RODI. (c) The GPS TEC data onboard Swarm. (d-e) The rate of change of TEC (ROT) and rate of change of TEC index (ROTI). The data from different GPS satellites are color-coded according to the PRN code in the colorbar on the right. (f) A map showing the field-of-view (red circle) of the GPS scintillation receiver at Ny-Ålesund (red dot), and the blue segment presents the Swarm orbit with an arrow showing the direction; the black circles and triangles show the piercing points of the GPS satellites tracked by the ground-based GPS receiver. (g-i) The GPS TEC, ROT and phase scintillation index (σ_ϕ) from the Ny-Ålesund GISTM receiver taking into account only GPS satellite data. The shaded area shows the time interval when Swarm A passes the field-of-view (red circle in panel f).*

Fig. 6 shows a comparison between ground-based measurements of the phase scintillation index (σ_ϕ) and the 4 selected parameters from Swarm A, namely RODI, ROTI, and the standard deviation of the electron density (std(Ne)) during the time interval when Swarm passes the field-of-view of Ny-Ålesund receiver, and the density gradient at 100 km scale. The irregularity parameters from Swarm are correlated with the ground-based phase scintillation strength, i.e., when RODI (ROTI, std(Ne), ∇Ne) increases, σ_ϕ increases as well. However, the relation is unlikely to be linear and therefore we do not make a linear fit as in Fig. 5.

Fig. 7 and Fig. 8 show the comparison between the ground-based GPS data (namely the amplitude scintillation index (S_4) and ROTI) and the Swarm datasets using the same format as Fig. 6. Both the amplitude scintillation index (S_4) and ROTI are loosely correlated with the Swarm derived irregularity parameters. This is to be expected, since S_4 is related to irregularities at scales of hundreds of meters, corresponding to a Fresnel scale [RD-03], while Swarm allows for detecting density gradients at km scales. Nevertheless, for large fluctuations in density observed by Swarm, we expect smaller scale fluctuations to be present as well, and thus a relation between the two quantities.

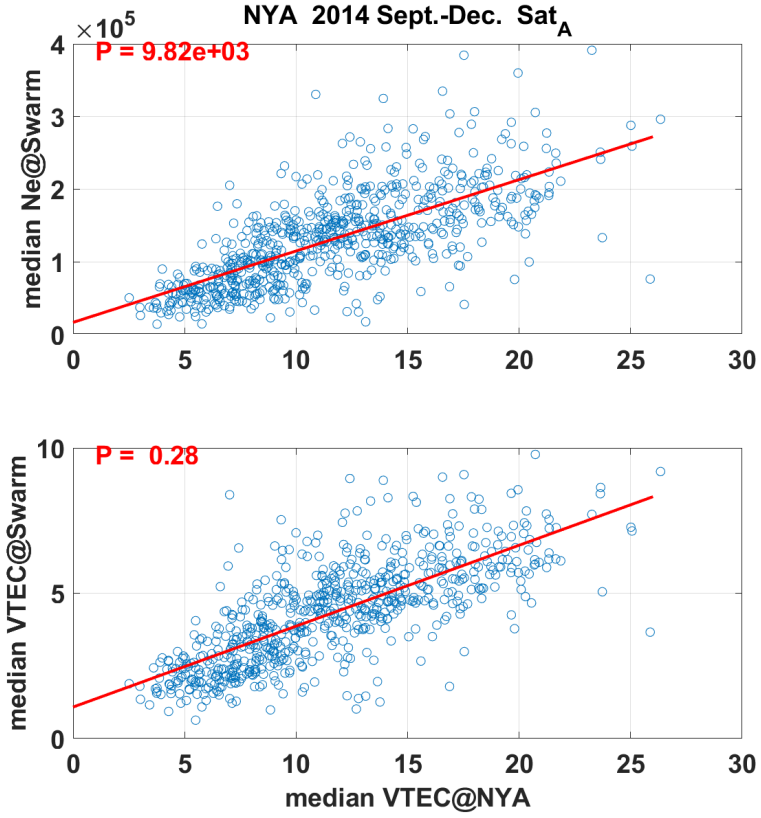

Fig. 5. Scatter plot of the VTEC from Ny-Ålesund versus VTEC and electron density from Swarm A. One circle in each plot represents one similar conjunction as the one in Fig. 4.

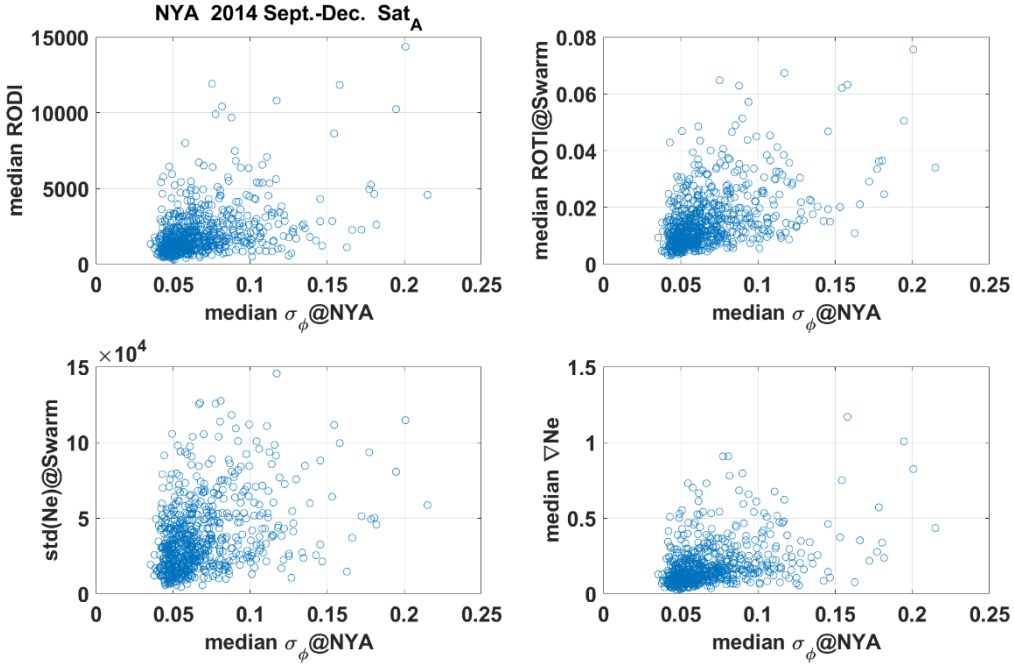

Fig. 6. Scatter plot of the phase scintillation index (σ_ϕ) from Ny-Ålesund versus selected parameters from Swarm A. Here one circle in each plot represents one conjunction in Fig. 4.

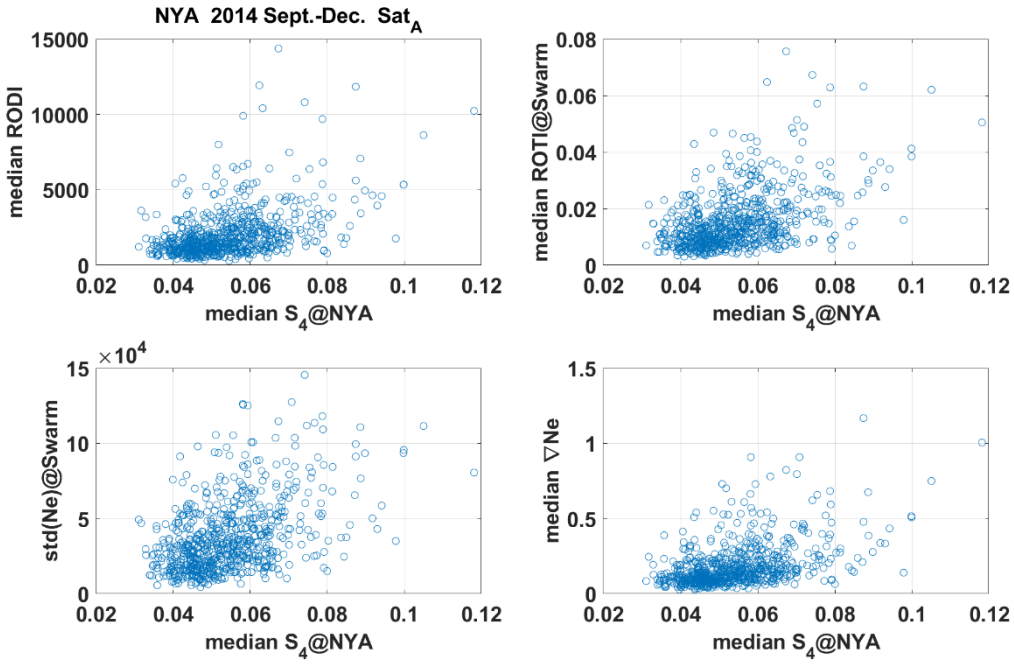

Fig. 7. Scatter plot of the amplitude scintillation index (S_4) from Ny-Ålesund station versus selected parameters from Swarm A.

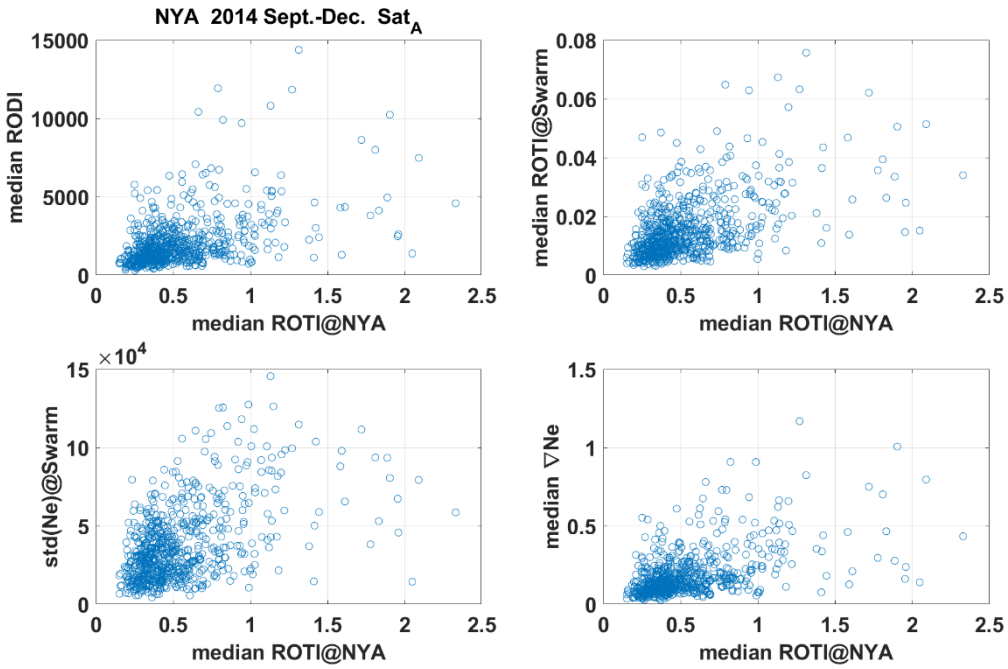

Fig. 8. Scatter plot of ROTI determined from GISTM at Ny-Ålesund station versus selected parameters from Swarm A.

4.3 Conjunction with the auroral station at Skibotn (SKN)

The GPS scintillation receiver at Skibotn is not continuously operated due to its remote location and maintenance issues. Fig. 9 shows operation times from 2014 to 2017. For comparison with Swarm, we use Skibotn data from Oct. 2014 to May 2015.

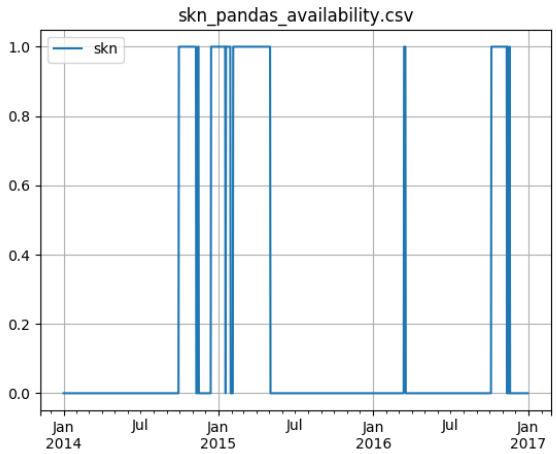

Fig. 9. Operation times of the Skibotn receiver: 1 indicates data available and 0 indicates no data.

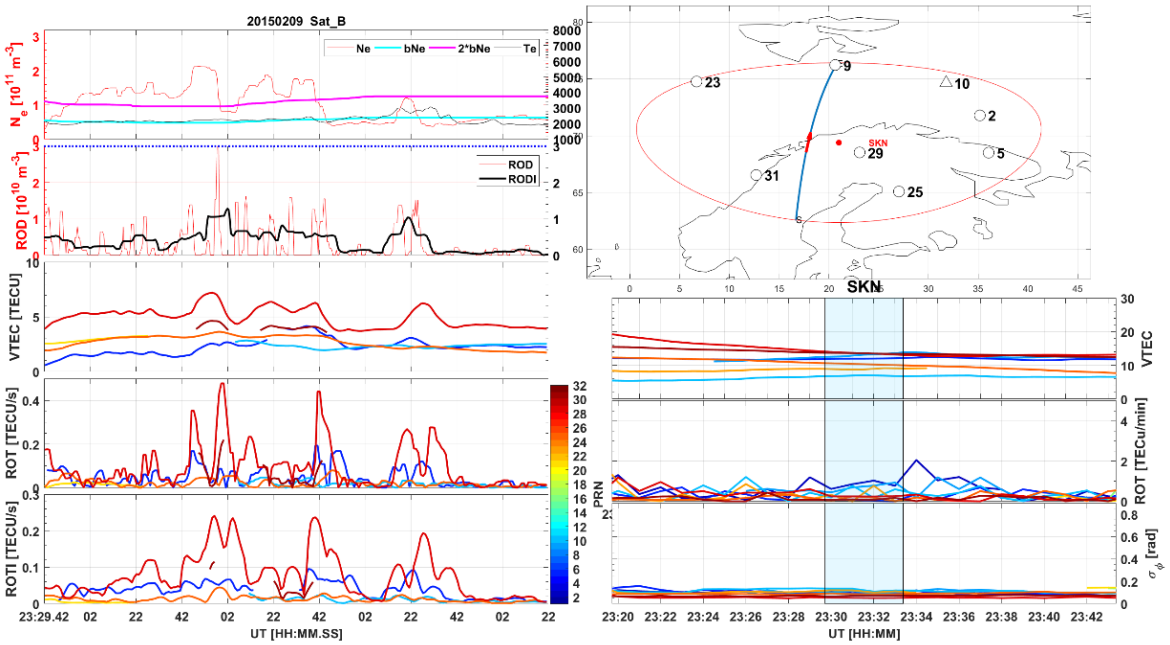

Fig. 10. Example of the conjunction of Swarm B and the ground-based GPS scintillation receiver at Skibotn. The figure is in the same format as Fig. 4.

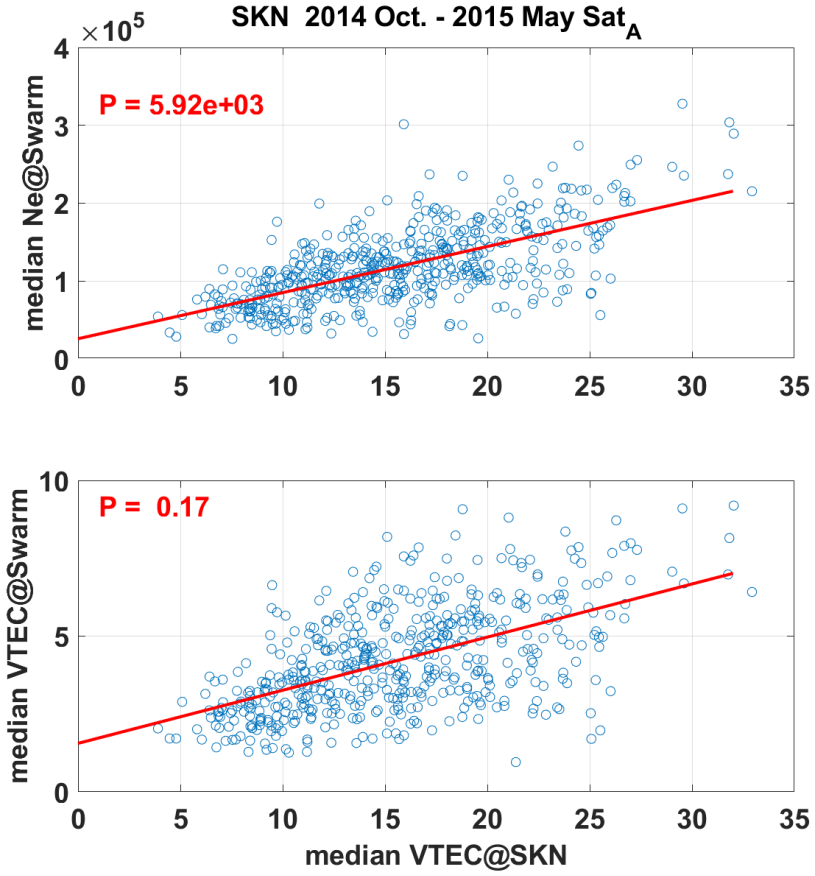

Fig. 11. Scatter plot of VTEC from Skibotn versus VTEC and electron density from Swarm A. One circle in each plot represents one similar conjunction as the one in Fig. 10.

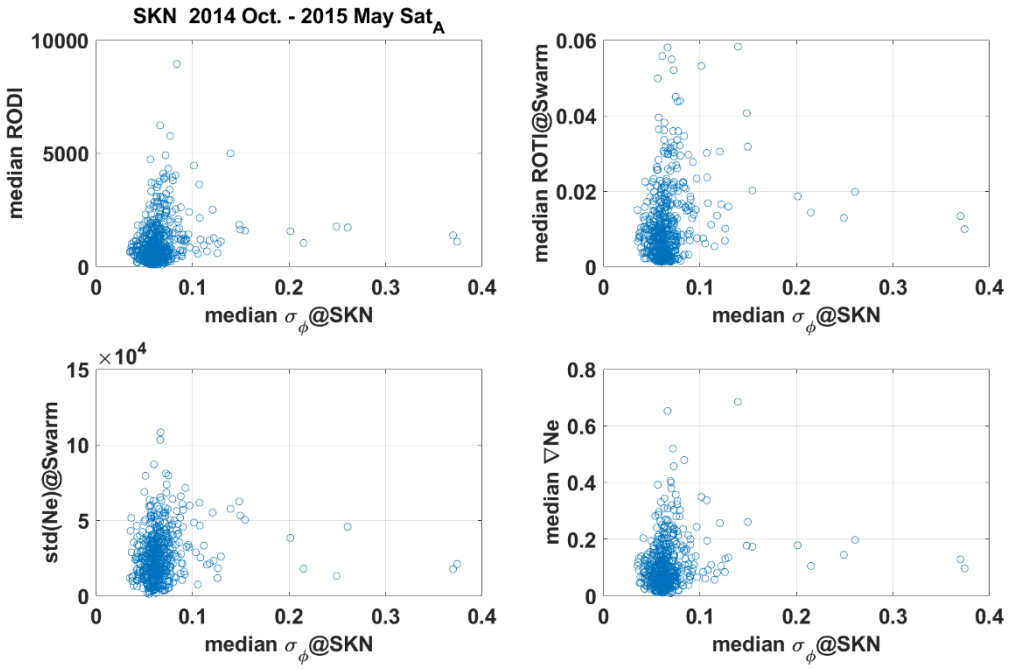

Fig. 12. Scatter plot of the phase scintillation index (σ_ϕ) from Skibotn versus selected parameters from Swarm A. Here one circle in each plot represents one conjunction similar to the one in Fig. 10.

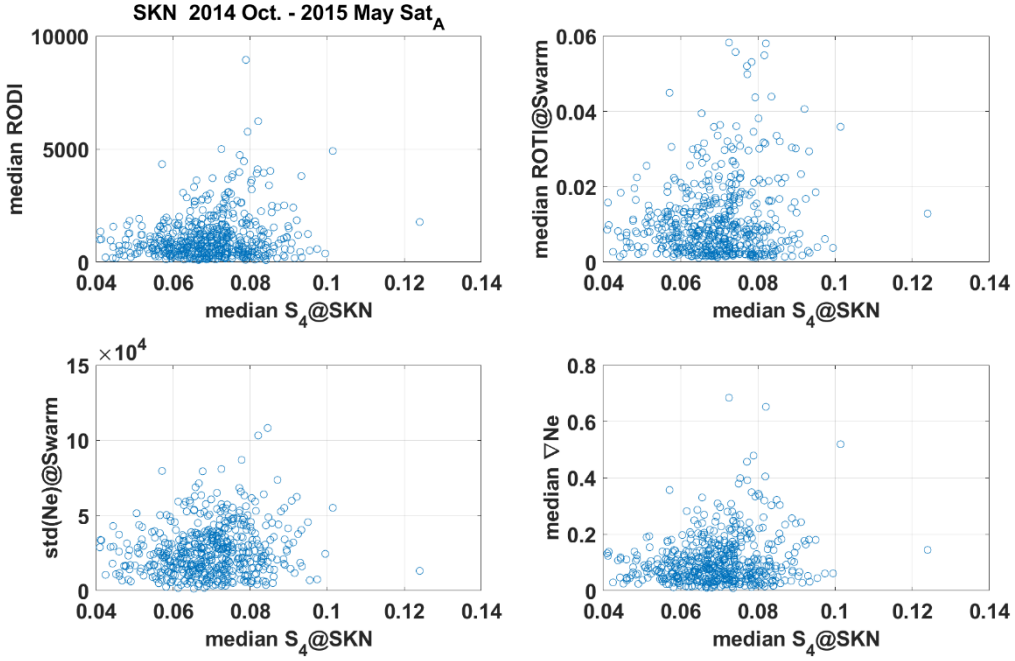

Fig. 13. The same format as Fig. 11 but for S_4.

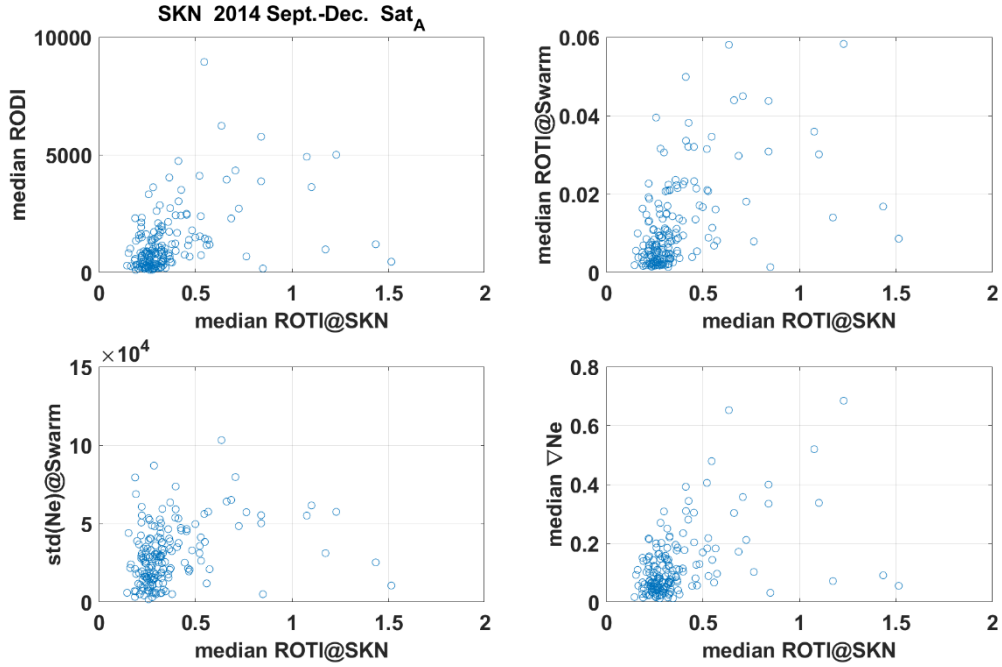

Fig. 14. The same format as Fig. 11 but for ROTI.

Analysing data from SKN station, it is evident that again for the auroral region, there is a good linear relationship between VTEC measurement on the ground and median VTEC and median Ne measured by Swarm. Better relationship between Ne and ground based TEC measurements are due to the fact that the density decreases with the altitude, and thus the local plasma density is more likely representative to the VTEC measured on the ground.

There is non-trivial relationship between median phase and amplitude scintillation index and parameters measured at Swarm. This is due to very dynamic ionosphere conditions in the auroral region, where the median scintillation index may not be representative for the actual conditions encountered by Swarm. In addition amplitude scintillations are not frequent at high latitudes. Finally, there is a relation between median ROTI measured at SKN and other parameteres (apart from std(Ne)) at Swarm.

4.4 Conjunction with the low-latitude station at SZT (ShenZhen)

ShenZhen is a low-latitude station near the magnetic equator (see Fig. 3), where the receiver can occasionally observe equatorial plasma bubbles. Fig. 15 shows the daily plot of the GPS data from ShenZhen on Sept. 10, 2014. From 12 UT to 19 UT(20-03 LT), the GPS TEC and ROT show clear variations, and the amplitude and phase scintillation indices show clear scintillations as well. These scintillations and ROT variations are likely to be caused by plasma bubbles. In Fig. 16 we show the conjunction with Swarm A. The electron density shows small plasma bubble (depletion in density) at around 16:36.30 UT, and the ROD, RODI, ROT, and ROTI all show significant variations with the plasma bubble.

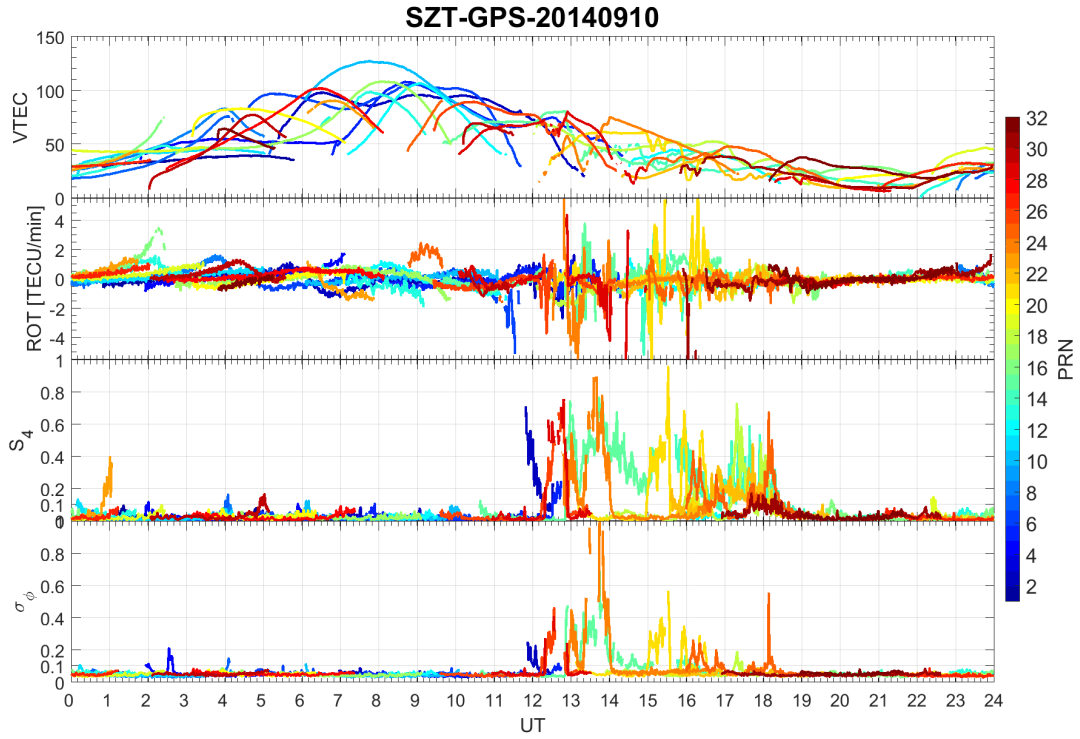

Fig. 15. Daily plot of (a) GPS TEC, (b) rate of change of TEC (ROT), (c) amplitude scintillation index (S_4), and (d) phase scintillation index (σ_ϕ) from SZT station.

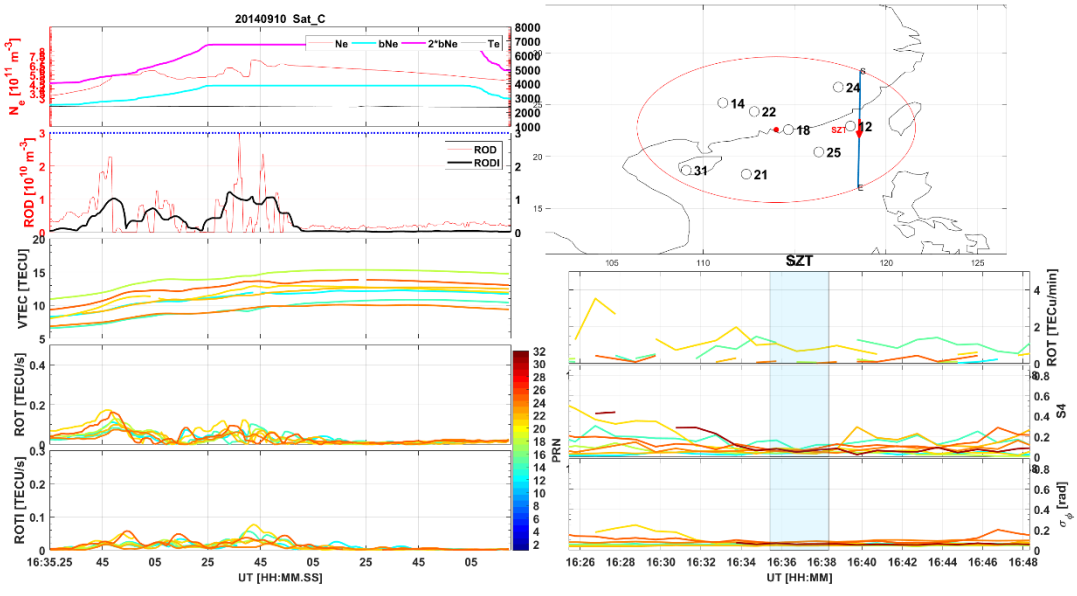

Fig. 16. An example of the conjunction of Swarm B and the ground-based GPS scintillation receiver at Shen-Zhen. The figure is in the same format as Fig. 4. The same day in Fig. 15 but for a shorter time interval.

We use GPS data from September to December 2014 to compare with the IPIR datasets. We only use ground-based GPS data above 30 degrees elevation angle and when the Swarm satellite passed the field-of-view for longer than 60 s. Fig. 17 show the scatter plot of VTEC from ShenZhen versus Ne as well as VTEC onboard Swarm. As ShenZhen is at low latitudes, the conjunction points are much fewer than the high-

latitude Ny-Ålesund station. For this reason, we plot the conjunctions with all the 3 Swarm satellites. Due to the similar orbit of Swarm A and C, the result for the two satellites are very similar. Fig. 17 shows the strong correlation between the 3 different datasets. It should be noted that the slopes between VTEC onboard Swarm and the VTEC from ground-based GPS receivers at ShenZhen and Ny-Ålesund are similar. However, the slopes between the in-situ Ne and the ground-based VTEC are quite different ($9.8x10^3$ at Ny-Ålesund versus at $1.9x10^4$ at ShenZhen), and this is likely related to the ionospheric profile and thickness at different ionospheric regimes (polar cap vs. equatorial region). Note that Ne and TEC onboard Swarm B are smaller than those from Swarm A and C. This is because that Swarm B is at higher altitude than Swarm A and C.

We also compare the four selected irregularity parameters from Swarm with the ground-based amplitude (S_4), phase scintillation (σ_ϕ) indices and ROTI in Fig. 18-20 which show loose correlation between the ground-based irregularity parameters and the space-based ones.

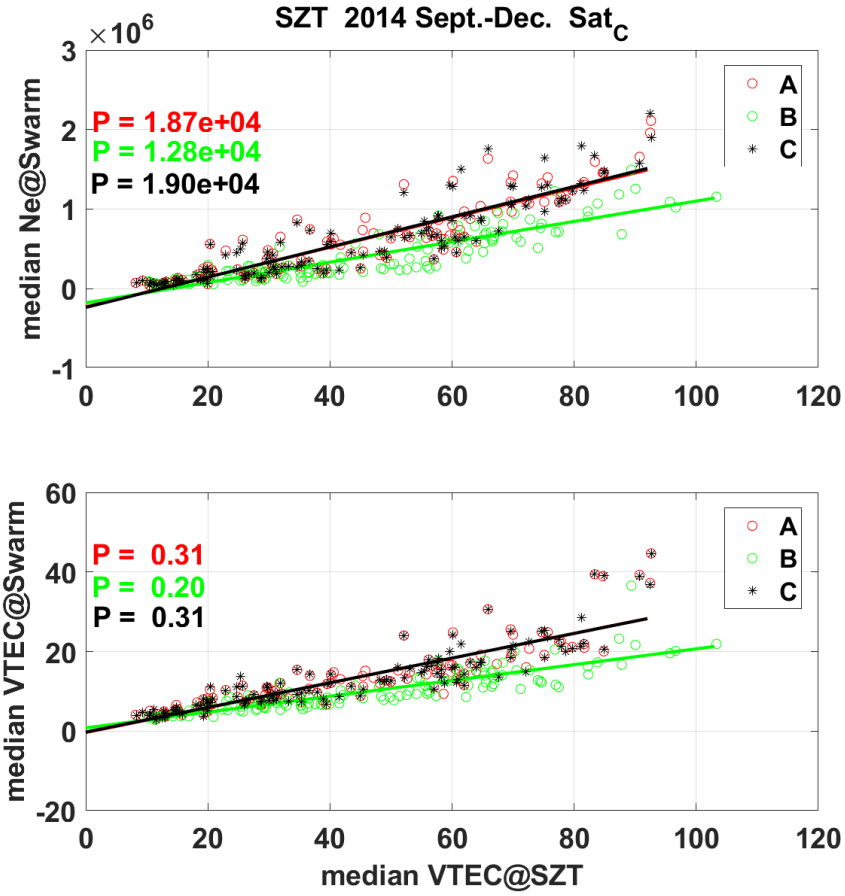

Fig. 17. Scatter plot of VTEC from SZT versus VTEC and electron density (Ne) from Swarm A. One circle in each plot represents one conjunction in Fig. 16. The results from different Swarm satellites are presented in different colors and symbols.

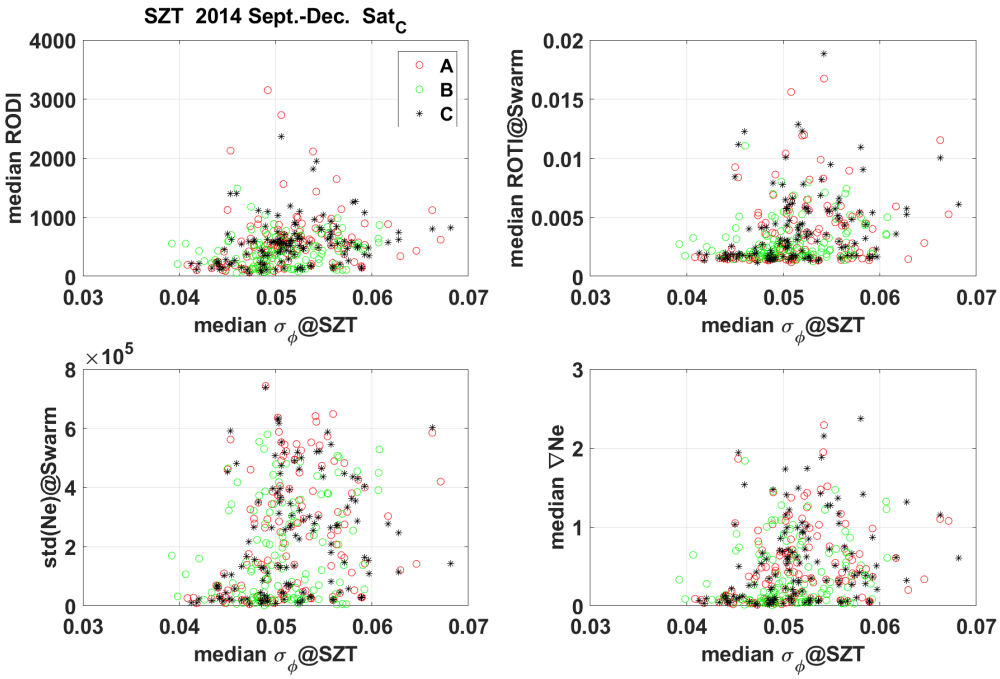

Fig. 18. Scatter plot of the phase scintillation index (σ_ϕ) from SZT versus selected parameters from Swarm A. Here one circle in each plot represents one conjunction in Fig. 16. The results from different Swarm satellites are presented in different colors and symbols.

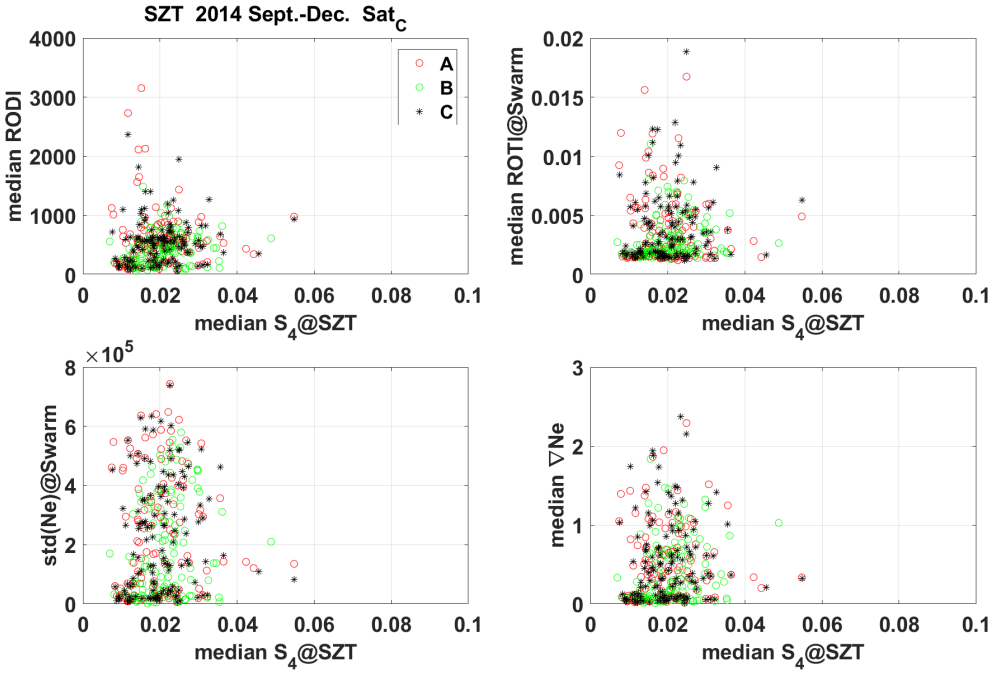

Fig. 19. The same format as Fig. 18 but for S_4.

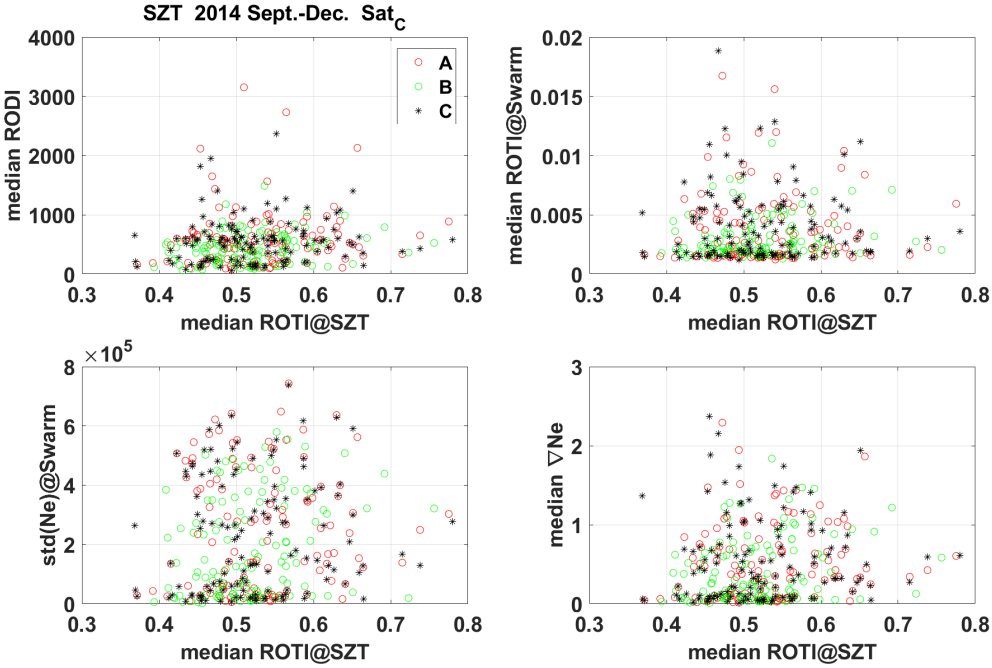

Fig. 20. The same format as Fig. 18 but for ROTI.

5 Discussion and conclusions

There is a good agreement between the median VTEC measured by the ground-based GISTM receivers at all considered geomagnetic latitudes and the VTEC as well as electron density measured by Swarm. The is a better linear relationship between the VTEC and electron density measured by Swarm due to the fact that VTEC measured by Swarm takes into account lower density, while VTEC measurements from the ground include the actual density values as measured by ground-based receivers.

The relationship between scintillation indices measured with the ground receivers and parameters derived from Swarm measurements is nonlinear. This is to be expected. Scintillations are the effect of scattering and diffraction of waves in the irregular medium, and in case of the amplitude scintillations, these irregularities are of the order of hundreds of meters, while Swarm can measure gradients at scales of larger than several km. Furthermore, the scattering and interference is not a linear function of irregularities, but an effect of those. Nevertheless, we do expect some relation between these parameters, and increase of scintillations with the activity, albeit not necessarily linear.

There is a near-linear relation between the ground-based measurements for ROTI and Swarm measurments of ROTI and RODI and variations in the electron density. This relation is very good at high latitudes, but not clear at mid-latitudes. It is as expected, since the geometry of the magnetic field, and the extent of the density variations along the magnetic field lines, makes it more likely that the variations observed by the ground-based observations are also experienced similarly by a satellite at high geomagnetic latitudes. At low latitudes, the variations can be within a horizontal layer above or below satellite.

To conclude, we compared the GPS data measured with the ground-based receivers with the IPIR datasets, and in particular new quantities. We selected three ground stations to present the different ionospheric regions, i.e., polar cap station at Ny-Ålesund (NYA), auroral station at Skibotn (SKN), and equatorial station in ShenZhen (SZT).

1. Data for ground-based VTEC from all stations considered shows good linear relation with in-situ electron density and VTEC onboard Swarm.
2. The relation between the ground-based scintillation indices (S_4 and σ_ϕ) and the Swarm derived irregularity parameters is not straightforward since scinitillations are the indirect result of irregularities, however we observe an increase in scintillations with an increase in ionospheric plasma disturbances.

***Acknowledgment**: We thank the Norwegian Polar Institute for assisting in GPS observations at Ny-Ålesund, and the Tromsø Geophysical Observatory for operating the receiver at Skibotn. Yaqi Jin thanks Prof. DongHe Zhang for providing GPS data from ShenZhen.*